ACS OMEGA

http://pubs.acs.org/journal/acsodf

Article

Distributed Activation Energy Modeling and Py-GC/MS Studies on Pyrolysis of Different Printed Circuit Boards for Resource Recovery

Jonnalagedda Varaha Jayarama Krishna, Peter Francis Prashanth, and Ravikrishnan Vinu*

Cite This: *ACS Omega* 2022, 7, 31713−31725

Read Online

ACCESS | Metrics & More | Article Recommendations | Supporting Information

ABSTRACT: Printed circuit boards (PCBs) constitute an important segment of electronic waste that can be effectively utilized to recover valuable metals and organics. The present work is focused on the kinetics and product distribution from pyrolysis of three different PCB samples, viz., television PCB (TV PCB), motherboard PCB (MB PCB), and hard disk PCB (HD PCB). The PCBs were pretreated to eliminate most of the metallic constituents. Kinetic analysis was performed using Vyazovkin's isoconversional method and distributed activation energy model (DAEM). The average apparent activation energies obtained from the Vyazovkin method were 207.2, 158.9, and 179.7 kJ mol^{-1} for the TV PCB, MB PCB, and HD PCB, respectively. The DAEM with five, four, and four pseudo-components was used to describe the decomposition kinetics of the TV PCB, MB PCB, and HD PCB, respectively. Importantly, two types of distributions, viz., Gaussian and Weibull, were utilized to effectively model the nonisothermal data obtained from thermogravimetric analysis at 10 and 20 °C min^{-1}. The evolution of pyrolysates belonging to functional groups such as phenolics, aromatics, aliphatics, halogenated compounds, N-containing compounds, and oxygenates was studied at two different temperatures (500 and 700 °C) using analytical pyrolysis−gas chromatograph/mass spectrometry (Py-GC/MS). The Py-GC/MS results demonstrated an increase in selectivity to aromatics and straight-chain aliphatics at 700 °C with a concomitant decrease in selectivity to phenols and oxygenates.

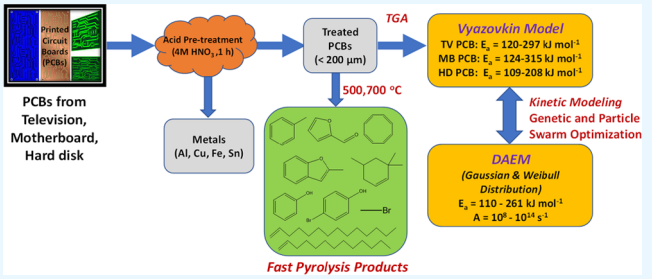

1. INTRODUCTION

The technological advancements during the last few decades in the electronic industry have led to rapid growth in the production and usage of various electronic devices. The production of new electrical and electronic devices and product obsolescence invariably led to the generation of electronic waste (e-waste). The worldwide generation of e-waste in 2019 was 53.6 million metric tons (MMT) and is expected to rise to 74 MMT by 2030.[1] India is the world's third-largest e-waste generator that produces 3.23 MMT of e-waste every year after China and USA.[2] Printed circuit boards (PCBs) are an indispensable part of any electrical and electronic equipment (EEE). The complex circuitry of PCBs encompasses various electrical components such as relays, capacitors, IC chips, timers, etc. This compounded arrangement in turn allows effective operation of any electrical equipment using a PCB. PCBs amount to nearly 6 wt % of the waste EEE (WEEE). In terms of recycling and environmental sustainability, it is difficult to process this highly heterogeneous component of e-waste, which is an amalgam of polymers, metals, and glass fibers. The treatment of PCBs is challenging mainly because of their complex structure and composition, which vary from one PCB to another.[3] Toxic materials, ranging from heavy metals such as Pb, Hg, and Pd to brominated flame retardants (BFRs) and adhesives, occupy a considerable fraction of PCBs and pose serious threat both to human health and the environment.[4,5]

Currently, most of the PCBs are either incinerated or landfilled. While incineration releases toxic fumes into the environment, landfilling of e-waste can lead to leaching of potentially hazardous materials into the environment.[6,7] Recently, thermochemical techniques have grown remarkably as an efficient methodology for treating e-waste, particularly PCBs. Pyrolysis is one such technique that produces solid char, liquid tar, and gases as the final products from a particular polymer or organic feedstock.[8−10] The advantage of pyrolysis of PCBs is that, if the temperature is high enough, it will melt the solder used for attaching the different components. Hence, the simultaneous recovery of the organic fraction and removal of the solder material will aid in the removal of the metallic fraction from the organic fraction.[11−13]

Thermogravimetric analysis (TGA) is widely used to study the thermal decomposition behavior and evaluation of kinetic

Received: April 1, 2022
Accepted: August 2, 2022
Published: August 31, 2022

parameters of a wide range of feedstocks, viz., biomass, algae, polymers, coal, and solid wastes. The mass loss and differential mass loss data are obtained using TGA at low heating rates of 5−100 °C min^{-1} as a function of time and temperature. The apparent kinetic parameters, viz., activation energy (E_a) and pre-exponential factor (A), are calculated using a number of isoconversional methods and model fitting techniques.[14−17] Rodriguez and co-workers[18,19] evaluated the kinetic behavior of slow pyrolysis of winery waste and agro-residues using Flynn−Wall−Ozawa (FWO) and distributed activation energy model (DAEM) methods. The average E_a values for winery wastes including grape marc and stalks were determined to be 123.1 and 189.7 kJ mol^{-1}, respectively, and those for agro-residues including plum pits, peach pits, and olive pits were determined to be in the range of 104.1−110.2 kJ mol^{-1}. The kinetics of PCB pyrolysis was studied using TGA by Kim et al.[17] A model-free Ozawa method was applied to calculate the activation energy, which varied in a broad range of 99.6−559.85 kJ mol^{-1} in the conversion range of 0.1−0.9.[17] Hao et al.[20] utilized the Coats−Redfern integral method to evaluate the reaction kinetics of PCBs. The kinetic parameters, E_a and A, were reported to be 205 kJ mol^{-1} and 3.09×10^9 min^{-1}, respectively, with a reaction order of 1.5. Chen et al.[21] studied the kinetics of nonmetallic fractions of PCBs using isoconversional methods and a discrete distributed activation energy model (DAEM). The authors identified 17 dominating reactions using the discrete DAEM with E_a and A varying in the range of 80.9−240.5 kJ mol^{-1} and 19−39.5 s^{-1}, respectively.[21] Krishna et al.[22] studied the copyrolysis kinetics of PCBs with keyboard keys, developed a DAEM using six pseudo-components following Gaussian distribution of activation energy, and obtained E_a and A in the range of 131.5−202 kJ mol^{-1} and 4.5×10^9−1.4×10^{13} s^{-1}, respectively.

Apart from evaluating the kinetics, it is imperative to study the product composition from pyrolysis of complex and heterogeneous PCBs. Quan et al.[23] studied the pyrolysis characteristics of woven glass fabric PCBs using thermogravimetry−Fourier transform infrared spectrometry (TG-FTIR) and pyrolysis−gas chromatography/mass spectrometry (Py-GC/MS) techniques. Three stages of decomposition were identified. The first stage (<293 °C) of decomposition produced H_2O, CH_4, HBr, CO_2, and acetone (CH_3COCH_3), while the products in the second stage (293−400 °C) were high-molecular weight organic compounds like bromophenols, bisphenol A, p-isopropenylphenol, and phenol. In the third stage (>400 °C), carbonization and char formation were observed. Kim et al.[17] studied the pyrolysis of phenolic paper-laminated PCBs using TGA and evolved gas analysis−MS to predict the kinetics and unravel the possible reaction pathways involved in PCB decomposition. The entire pyrolysis process was divided into four zones, viz., zone 1, where vaporization of phosphorus flame retardants (100−280 °C) was observed; zone 2, where pyrolysis of laminated paper and tetrabromo bisphenol A (TBBA) (280−370 °C) occurred; zone 3, where pyrolysis of phenolic resin (370−500 °C) occurred; and zone 4, where char stabilization with the release of aromatic compounds (>500 °C) was observed. Duan and Li[24] studied the pyrolysis behavior of PCB assembly (PCBA) obtained from video cards using Py-GC/MS. The PCBA was dismantled into the substrate, integrated circuit (IC), and plastic slot. The pyrolysis products derived from the substrate were acetone, bromotoluene, phenol, and 3-methyl-2,3-dihydro-1-benzofuran. The compounds obtained from IC pyrolysis were acetone, phenol, 2-methyl-phenol, and 2,5-dimethyl-phenol, while those from the plastic slot were mainly benzoic acid and benzene homologues.

A few studies in the literature have focused on improving the selectivity of specific chemicals and the quality of pyrolysis vapors. The microwave-assisted pyrolysis of waste PCBs was studied by Suriapparao et al.[13] using carbonaceous suspectors such as graphite and activated carbon. The authors reported an increase in the selectivity to phenol (>90%) in the tar fraction with the use of high amounts of susceptor (10:50 g/g of PCB:susceptor). The pyrolysis studies of PCB, coal powder, and their mixtures were investigated by Hao et al.[20] using TGA and FTIR spectroscopy. It was observed that the addition of 40 wt % coal improved the quality of pyrolysis vapors. The intensity of the characteristic absorption peak of HBr at 2500−2750 cm^{-1} was very low, as the coal powder effectively solidified the bromine molecules to settle down in the residue. During the copyrolysis of inorganic-rich PCBs with organic-rich keyboard keys of different mixture compositions, it was shown that the formation of oxygenated organics was mitigated, while the aromatic hydrocarbons and nitrogen-containing aromatics dominated the pyrolysates.[22]

Pyrolysis is an effective thermochemical treatment for resource and energy recovery from PCBs. Several value-added chemicals such as aromatics, plastic monomers, combustible gases, and a wide range of unoxidized metals can be extracted. To design a thermochemical reactor at an industrial scale, it is important to understand the kinetics and various functionalities present in different PCB samples. In the current study, a multidistribution DAEM is employed to understand the kinetic behavior and overall pyrolysis mechanism of PCB samples derived from three different sources, viz., television PCB (TV PCB), motherboard PCB (MB PCB) and hard disk PCB (HD PCB). The objectives of this study are twofold. The first one is to unravel the kinetics and decomposition behavior of three PCB samples using the advanced isoconversional Vyazovkin method and DAEM. The activation energy as a function of conversion is computed using the Vyazovkin method, which uses numerical integration to improve the accuracy of the solution. The activation energy values obtained from the Vyazovkin method serve as a basis to perform the DAEM to obtain the kinetic and statistical parameters for the pyrolysis of PCB samples. The second one is to study the product composition from the pyrolysis of three PCB samples using Py-GC/MS under fast pyrolysis conditions. The key novelty of this study is the inclusion of two different distributions, viz., Gaussian and Weibull, in a DAEM to accurately model the complex nonisothermal pyrolysis behavior of PCBs.

2. EXPERIMENTAL SECTION

2.1. Materials and Methods. The TV PCB was purchased from a TV repair shop in Chennai, while the MB PCB and HD PCB were collected from the dump yard of the IIT Madras campus where all the e-wastes are stored before being sold out. With the help of a cutting tool, all the samples were chopped and hand-cut into small pieces. These small pieces were then made into a fine powder using a planetary ball mill (Fritsch Pulverisette 5) and a household mixer grinder (Preethi Blue Leaf, MG 214/002) in sequence. The rotating speed of the ball mill was 400 rpm. The size reduction processes were carried out for a period of 10−20 min. The size of the final powder obtained was <200 μm. A small particle size

https://doi.org/10.1021/acsomega.2c02003
ACS Omega 2022, 7, 31713−31725

is preferred to minimize the influence of heat and mass transfer effects that would normally be present across a larger particle size or chunk of materials. This ensured that the rate of the reaction is influenced by only reaction kinetics.[25] Before analysis, the PCBs were dissolved in concentrated nitric acid (4 M) to extract the metals from the circuit boards. Nitric acid treatment is shown to dissolve a number of metals in PCBs including copper.[26] The concentration of nitric acid used in this study is in line with that in the literature.[26] The raw PCBs were labeled as untreated samples, while the ones subjected to acid pretreatment were labeled as treated samples.

The proximate analysis of the PCBs was done using a TGA (Model 2000A, Navas Instruments) according to the ASTM E1131−08 method. The CHNS elemental analysis of the samples was performed using a Thermo Flash 2000 organic elemental analyzer (Thermo Fisher Scientific). The higher heating values (HHVs) were determined using an isoperibolic bomb calorimeter (IKA C2000, Germany). The composition of various metals present in PCB samples was analyzed using an inductively coupled plasma optical emission spectrometer (ICP-OES) (Perkin Elmer Optima 5300 DV ICP-OES). Before analysis, the metals in the PCB were dissolved by adding 3:1 (vol./vol.) HCl:HNO_3 solution to ∼0.25 g of pyrolysis residue. This pyrolysis residue is a complex amalgamate of metals, aromatized polymeric residues, and glass fibers. The greenish color of the solution confirmed the dissolution of metals.[13,22] The solution was then diluted to 50 mL, the carbonaceous matter was removed by passing the solution through a 5 μm filter, and the filtrate was analyzed to determine the composition of various metals. The ICP-OES analysis of the untreated and acid-pretreated PCB samples was performed two times, and the average and standard deviation values are reported.

TGA of the PCB samples was performed in an SDT Q600 TG analyzer (T.A. Instruments) in an inert ambience with a 100 mL min^{-1} flow of N_2 gas. An alumina crucible was placed on the cantilever beam of the TGA instrument, to which a mass of 3 ± 0.25 mg of the PCB sample was weighed. The samples were subjected to multiple heating rates (10, 20, 30, and 40 °C min^{-1}). Higher heating rates were not employed due to the higher thermal lag between the furnace and sample temperatures, which would affect the kinetic calculations. The crucibles were combusted at 850 °C in a muffle furnace after each run to ensure that organic matter was not present before the start of the subsequent experiment.

2.2. Analytical Pyrolysis−Gas Chromatography/Mass Spectrometry (Py-GC/MS). The composition of the pyrolysates, which contain devolatilization products and gaseous products, was determined by performing experiments in a Pyroprobe 5200 pyrolyzer (CDS Analytical) interfaced with GC/MS (Agilent Technologies, 7890−5975C). The typical heating rate of the polymeric sample matrices in the Pyroprobe is shown to be 125−150 °C s^{-1}.[27,28] This shows that this setup involves a fast heating rate as compared to TGA. The PCB samples (300 ± 10 μg) were placed in a quartz tube and placed inside the Pt-coil filament. This was then subjected to the desired pyrolysis temperature (500, 700 °C), and held for 30 s. A number of studies in the literature have demonstrated that a steady conversion is achieved for a variety of polymers and biomass samples within 30 s in a Pyroprobe reactor at temperatures above 500 °C.[27−30] Moreover, the maximum evolution of pyrolysis vapors is shown to occur around 10−15 s using Pyroprobe−Fourier transform infrared spectroscopy experiments, and by 30 s, the generation of vapors is nearly complete.[27−30] The organic compounds in the pyrolysate were separated by passing them through a HP-5MS (30 m × 0.25 mm i.d. × 0.25 μm film thickness) capillary column. The GC column oven temperature was maintained initially at 40 °C for 1 min, followed by a ramp of 5 °C min^{-1} to 280 °C, and finally maintained at this temperature for 10 min. The inert gas used for pyrolysis and the carrier gas used for GC/MS were both ultrahigh-pure helium (99.9995%). It was flown through the column at a flow rate of 1.2 mL min^{-1} with a split ratio of 100:1. The pyrolysis vapors were scanned in the mass range (m/z) of 50−500 Da at an electron ionization voltage of 70 eV. The transfer line between the Pyroprobe and GC/MS was maintained at 300 °C to avoid condensation of pyrolysates. The GC/MS interface and ion source temperatures were maintained at 300 and 250 °C, respectively. The mass spectra of the pyrolysates were matched with the NIST library, and the pyrolysate composition is reported in terms of relative peak area % (or selectivity %). The compounds with a high match factor (>85%) were considered for the composition analysis. Each experiment was repeated three times, and the yields reported are the average values with a standard deviation of 5−7%.

3. KINETIC ANALYSIS

3.1. Isoconversional Model. PCB pyrolysis occurs in multiple steps owing to its complex structure.[22,31−33] The reaction kinetics can be described using the following equation[14,22,34]

$$\frac{d\alpha}{dT} = \frac{A}{\beta} e^{-E_a/RT} f(\alpha) \quad (1)$$

The above-mentioned expression, when rearranged and integrated, gives the following equation[14,35]

$$g(\alpha) = \int_0^\alpha \frac{d\alpha}{f(\alpha)} = \frac{A}{\beta}\int_0^T e^{-E_a/RT} dT = \frac{A}{\beta} I(E_\alpha, T_{\alpha,i}) \quad (2)$$

Even though analytical approximations can be applied to the temperature integral in eq 2 to obtain rate equations from which the rate parameters can be calculated by linear regression, the numerical integration of the integral is shown to yield the accurate prediction of rate parameters.[14] Therefore, the integral is transformed to eq 3, which can be solved numerically according to the advanced isoconversional method of Vyazovkin.

$$\left| n(n-1) - \sum_{i\neq j}^{n}\sum_{j}^{n} [I(E_\alpha, T_{\alpha,i})\beta_j]/[I(E_\alpha, T_{\alpha,j})\beta_i] \right| = \min \quad (3)$$

The above-mentioned expression is a nonlinear optimization problem, which was solved using MATLAB by setting the lower and upper bounds of activation energy to 20 and 350 kJ mol^{-1}, respectively. The genetic algorithm module of MATLAB was used to evaluate the dependence of activation energy on conversion.

3.2. DAEM. The extent of conversion defined by the DAEM is given by the following equation[36−38]

https://doi.org/10.1021/acsomega.2c02003
ACS Omega 2022, 7, 31713−31725

Table 1. Characterization of Untreated and Treated PCB Samples

sample	ultimate analysis (wt % db)				proximate analysis (wt % db)			HHV (MJ kg^{-1})
	C	H	N	[a]O	volatile matter	fixed carbon	ash	
Untreated Samples								
TV PCB	51.2 ± 0.7	6.2 ± 0.7	3.5 ± 0.1	33.4 ± 1.4	71.5 ± 2.2	22.8 ± 0.7	5.7 ± 1.6	26.5 ± 1.4
MB PCB	27.8 ± 0.4	2.6 ± 0.02	1.2 ± 0.08	1.1 ± 0.5	32.7 ± 0.3	0	67.3 ± 0.3	13.6 ± 0.5
HD PCB	25.3 ± 0.9	2.3 ± 0.2	0.8 ± 0.04	0.2 ± 0	28.6 ± 0.1	0	71.4 ± 0.1	13.3 ± 0.9
Treated Samples								
TV PCB	48.4 ± 0.2	5.4 ± 0.1	3.7 ± 0.1	41 ± 0.6	76.5 ± 0.6	22 ± 0.1	1.5 ± 0.7	23.9 ± 0.8
MB PCB	26.2 ± 0.4	2.5 ± 0.1	1.3 ± 0.2	10.2 ± 0.9	40.2 ± 0.9	0	59.8 ± 0.9	12.9 ± 1.2
HD PCB	24.8 ± 0.7	2.4 ± 0.5	0.7 ± 0.1	11.5 ± 1.3	39.4 ± 0.7	0	60.6 ± 0.1	13.4 ± 0.7

[a]% O = 100 − % C − % H − % N − % S − % Ash (sulfur was not detected in the samples); db—dry basis.

$$\alpha(T) = \sum_{i=1}^{n} c_i - \int_0^{\infty} \exp\left[-\int_{T_0}^{T} \frac{A}{\beta} \exp\left(-\frac{E}{RT}\right) dT\right] f(E) dE \quad (4)$$

The conversion is normalized with respect to the amount of the residue formed such that it varies from zero to 100%. Equation 4 assumes that first-order kinetics is applicable for the decomposition of the pseudo-components. The first-order reaction model is shown to be valid for a wide variety of polymeric materials including lignocellulosic biomass, its biochemical components like cellulose, hemicellulose, and lignin, and plastics such as polypropylene, poly(ethylene terephthalate), and polycarbonate. More importantly, increasing the reaction order is known to broaden the reaction profile and skew it to higher temperatures.[39,40] Moreover, the pre-exponential factor is usually assumed to be a constant for the decomposition of a specific pseudo-component, while its reactivity distribution is described by a continuous distribution of activation energy. This is typical for the pyrolysis of a wide variety of lignocellulosic biomass and polymer pyrolysis.[39,40] Nevertheless, the pre-exponential factor can also be assumed to have a power law dependency on temperature or follow the kinetic compensation effect.[39] The assumption of constant A for a pseudo-component also limits the number of fitted parameters in a DAEM.

By differentiating eq 4 with respect to T, the following expression is obtained

$$\frac{d\alpha}{dT} = \sum_{i=1}^{n} c_i \int_0^{\infty} \frac{A}{\beta} \exp\left[-\frac{E}{RT} - \int_{T_0}^{T} \frac{A}{\beta} \exp\left(-\frac{E}{RT}\right) dT\right] f(E) dE \quad (5)$$

The composition factor (c_i) in eqs 4 and 5 represents the volatiles produced by decomposition of the respective pseudo-components. The activation energy distribution, $f(E)$, is given by the following expressions

$$f(E) = \frac{1}{\sigma\sqrt{2\pi}} \exp\left[\frac{-(E - E_0)^2}{2\sigma^2}\right] \quad (6)$$

$$f(E) = \frac{\phi}{\eta}\left(\frac{E - \gamma}{\eta}\right)^{\phi - 1} \exp\left(-\left(\frac{E - \gamma}{\eta}\right)^{\phi}\right) \quad (7)$$

eq 6 represents the Gaussian distribution function, and eq 7 is the Weibull distribution function. The former is used when the activation energy of a set of reactions follows a symmetric shape, while the latter is used to account for the asymmetries in the family of reactions.[39,41] In eq 6, E_o and σ represent the mean activation energy and the standard deviation, respectively, while in eq 7, ϕ, η, and γ denote the shape parameter, scale parameter, and location parameter, respectively.

The E_o and σ for a Weibull distribution function are given by the following equations

$$E_o = \gamma + \eta\Gamma\left(\frac{1}{\phi} + 1\right) \quad (8)$$

$$\sigma = \eta\left(\Gamma\left(\frac{2}{\phi} + 1\right) - \Gamma\left(\frac{1}{\phi} + 1\right)^2\right)^{0.5} \quad (9)$$

As the inner integrals of eqs 4 and 5 do not have an exact analytical solution, the following expression is used to approximate the inner integral.[42]

$$g(T) = \int_0^{T} \exp\left(-\frac{E}{RT}\right) dT = \frac{RT^2}{E} \exp\left(-\frac{E}{RT}\right) \frac{0.99954E + 0.58058RT}{E + 2.54RT} \quad (10)$$

3.2.1. Numerical Method for Parameter Estimation. The kinetic parameters (A, E_0, σ, c_i, γ, ϕ, η) were determined using an objective function based on the conversion rate $\left(\frac{d\alpha}{dT}\right)$ as defined by eq 11

$$S = \sum_{i=1}^{n_d} \left[\left(\frac{d\alpha}{dT}\right)_{i,\exp} - \left(\frac{d\alpha}{dT}\right)_{i,\mathrm{cal}}\right]^2 \quad (11)$$

The objective function of eq 11 does not have an explicit solution. The above-mentioned equation was solved using the particle swarm optimization (PSO) technique of MATLAB.[43] The fitness parameter shown in eq 11 was evaluated by comparing the simulated $\left(\frac{d\alpha}{dT}\right)$ curve obtained using the optimized kinetic parameters with that of the experimental curve obtained from TGA experiments.

$$\mathrm{Fit}(\%)_{\mathrm{DTG}} = \left(1 - \frac{\sqrt{\frac{S}{n_d}}}{\left(\frac{d\alpha}{dT}\right)_m}\right) \times 100\% \quad (12)$$

where $\left(\frac{d\alpha}{dT}\right)_m$ is the maximum experimental value.

The similar objective function (S^1) and fitness parameter, $\mathrm{Fit}(\%)_{\mathrm{conv.}}$, are defined by eqs 13 and 14 to calculate the fitness parameter for conversion curves, respectively.

https://doi.org/10.1021/acsomega.2c02003
ACS Omega 2022, 7, 31713−31725

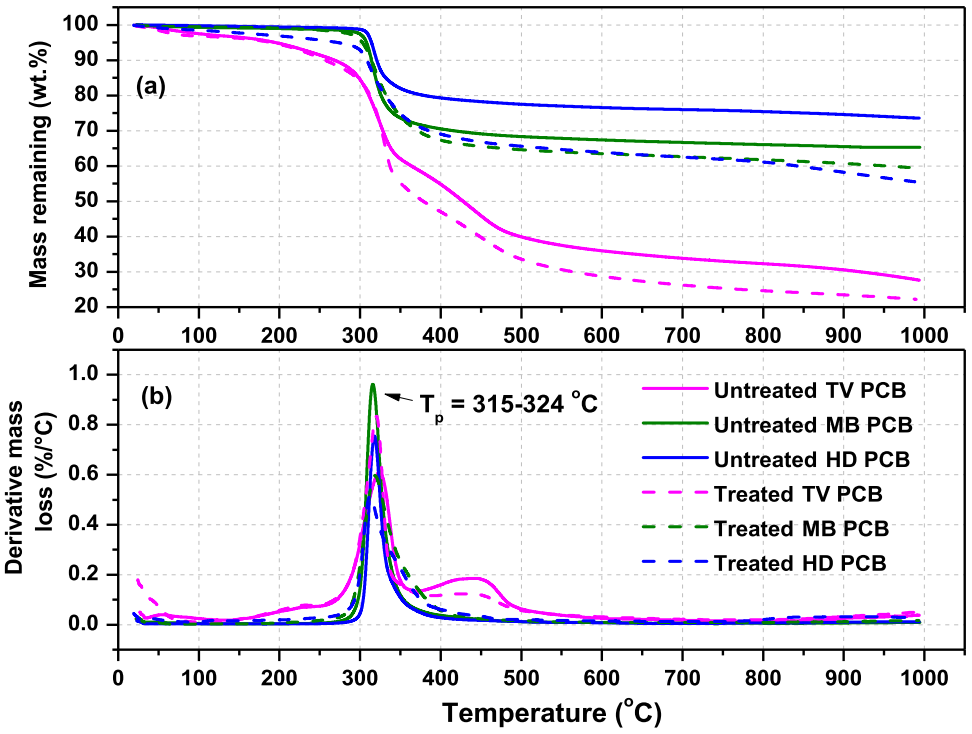

Figure 1. (a) Thermogravimetric (TG) mass loss and (b) differential thermogravimetric (DTG) curves for the TV PCB, MB PCB, and HD PCB at 10 °C min^{-1}.

Table 2. Composition of Metals Present in Ash of PCB Samples[a]

	untreated samples (wt % in ash)			treated samples (wt % in ash)	
metals	TV PCB	MB PCB	HD PCB	MB PCB	HD PCB
aluminum (Al)	1.5 ± 0.2	3.2 ± 0.3	2.34 ± 0.3	0.5 ± 0.05	0.07 ± 0.05
copper (Cu)	38.4 ± 3.0	66.3 ± 4.0	60.6 ± 4.5	3.2 ± 0.3	2.6 ± 0.3
iron (Fe)	2.68 ± 0.3	0.22 ± 0.03	0.28 ± 0.05	n.d.	n.d.
nickel (Ni)	1.1 ± 0.1	0.7 ± 0.1	0.43 ± 0.05	n.d.	n.d.
lead (Pb)	2.38 ± 0.2	1.25 ± 0.1	0.82 ± 0.1	n.d.	n.d.
tin (Sn)	3.43 ± 0.3	1.05 ± 0.1	0.98 ± 0.1	n.d.	n.d.

[a]No detectable amount of the metals was obtained in the treated TV PCB.

$$S^1 = \sum_{i=1}^{n_d} [(\alpha)_{i,\mathrm{exp}} - (\alpha)_{i,\mathrm{cal}}]^2 \quad (13)$$

$$\mathrm{Fit}(\%)_{\mathrm{conv.}} = \left(1 - \sqrt{\frac{S^1}{n_d}}\right) \times 100\% \quad (14)$$

4. RESULTS AND DISCUSSION

4.1. Characterization and TGA of PCBs. The basic characterization of the treated PCB samples is presented in Table 1. From Table 1, it can be observed that the volatile content of the TV PCB is higher than that of the other two PCBs both before and after the acid treatment. The inherent ash content in the untreated TV PCB is low (5.7%) as compared to that of other PCBs (67−71 wt %). The key difference in the ash content is mainly because TV PCBs are single-layered, while MB PCBs and HD PCBs are multilayered in design where high concentrations of metals and glass fibers are used. The carbon content of TV PCBs is similar to that given by Chiang et al.[44] who investigated the pyrolysis characteristics of IC boards at various particle sizes and temperatures.

The low HHV of the MB PCB and HD PCB can be attributed to the lower carbon content compared to that of the TV PCB. The proximate and ultimate analysis results suggest that there are significant differences in the composition and structure of the TV PCB compared to the MB PCB and HD PCB. Moreover, the fixed carbon of the TV PCB is intact even after the acid treatment, which shows that the acid wash primarily attacks the inorganics in the PCB. The chemical formulae of the treated TV PCB, MB PCB, and HD PCB derived from elemental analysis are given by $C_4H_{5.4}O_{2.6}$, $C_{2.2}H_{2.5}O_{0.64}$, and $C_2H_{2.4}O_{0.72}$, respectively. On comparing the volatile matter content of the feedstocks, it can be suggested that the TV PCB, being rich in the volatile fraction and carbon along with low inorganic matter, is a potential feedstock to produce a high yield of pyrolysis oil compared to the MB PCB and HD PCB.

The experimental mass loss and derivative mass loss profiles of untreated and treated PCB samples at 10 °C min^{-1} are presented in Figure 1a,b. The TG and DTG graphs at 20, 30, and 40 °C min^{-1} for the treated samples are shown in Figures

https://doi.org/10.1021/acsomega.2c02003
ACS Omega 2022, 7, 31713−31725

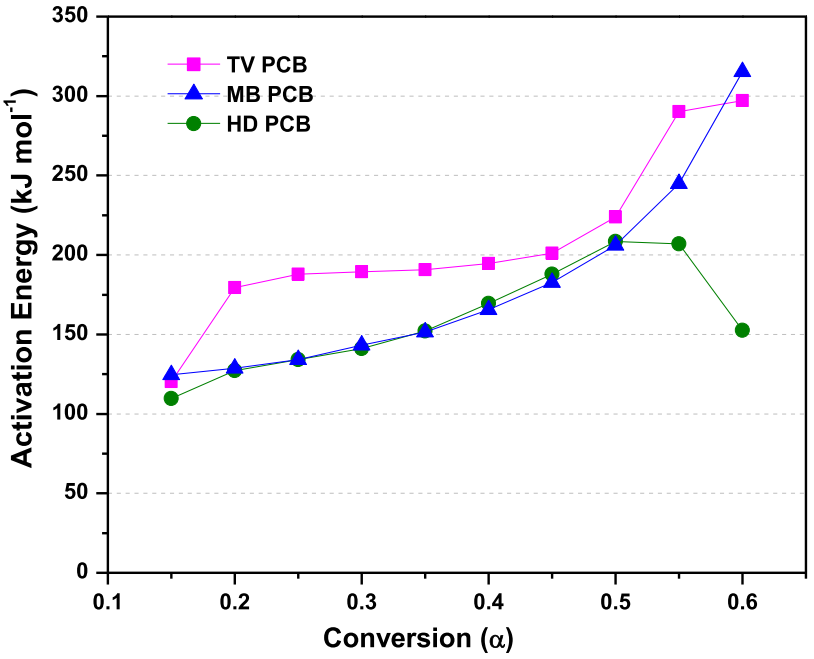

Figure 2. Variation of activation energy with respect to conversion for the TV PCB, MB PCB, and HD PCB.

S1−S3 (Supporting Information). The char obtained at the end of the pyrolysis process from treated samples was 22.5, 59.4, and 56 wt % for the TV PCB, MB PCB, and HD PCB, respectively. These values are in reasonable agreement with the sum of fixed carbon and ash of these samples analyzed using a proximate analyzer. Importantly, the mass loss curves show that the acid pretreatment tends to decrease the amount of residual char. At 980 °C, the reduction in the mass of the residue was 24% for the HD PCB, 20% for the TV PCB, and ∼8% for the MB PCB. This shows the leaching of metals from the PCB due to acid treatment. The composition of the key metals present in the PCB samples before and after the acid pretreatment is presented in Table 2. A high concentration of copper is observed in the raw MB PCB (66.3%) and raw HD PCB (60.6%) as compared to that in the TV PCB (38.4 wt %). The acid pretreatment tends to completely remove Fe, Ni, Pb, and Sn from all the PCBs, while significantly reducing Cu and Al. No detectable amount of Cu was found in the treated TV PCB.

It can be observed from Figure 1b that the TV PCB exhibits three distinct regions of decomposition, viz., 150−250, 250−400, and 400−600 °C, while the MB PCB and HD PCB showed only one major decomposition in the temperature range of 300−450 °C. This implies that the decomposition pattern is influenced by the composition, structure, and origin of PCB samples. Chiang et al.[44] reported two stages of degradation during the pyrolysis of IC boards, viz., 287−307 and 357−507 °C. Grause et al.[45] reported three stages of degradation for paper-laminated PCBs with the first stage observed from ambient to 270 °C, the second stage observed between 270 and 370 °C, and the third stage observed above 370 °C. Chen et al.[21] studied the nonmetallic fraction of PCBs and described the entire decomposition in three stages. The first, second, and third stages are reported to occur at 20−98, 98−570, and 570−800 °C, respectively.

In the present work, the pyrolysis behavior of the three PCBs can be classified as follows. The first stage, which corresponds to a low-temperature region typically below 100 °C, is mainly attributed to the removal of the physisorbed moisture from the samples. The second stage, where active pyrolysis happens, is characterized by the decomposition in the range of 100−600 °C. The maximum mass loss can be observed in the second stage, which is primarily due to the devolatilization of epoxy resins from the PCB samples. The third stage corresponds to high temperatures (600−1000 °C) and is characterized by a minor mass loss of 6−10 wt %, particularly due to the decomposition of char present in the PCB samples. The temperature of maximum decomposition (T_p) as observed in Figures 1 and S1−S3 (Supporting Information) varied in the range of 321−344, 318−350, and 313−345 °C when the sample heating rates were 10, 20, 30, and 40 °C min^{-1}. The increase in T_p toward higher values can be attributed to the fact that the time taken by the inert gas to attain equilibrium with the samples is considerably longer at high heating rates. At higher heating rates, the temperature difference between the surface and the center of the sample particles increases due to the lower thermal energy accumulation required for bond breaking. This subsequently leads to a shift in the rate of maximum mass loss to a higher temperature. The TG experiments carried out at different heating rates aid in understanding the decomposition phenomena better. They also aid in calculating the kinetic parameters for the conceptualization and design of an industrial pyrolysis reactor for effective treatment of PCB samples originating from different sources, and e-wastes in general.

4.2. Evaluation of Kinetic Parameters. *4.2.1. Vyazovkin Method.* The change in the apparent activation energy as a function of conversion is shown in Figure 2. The sum of square errors (SSE) calculated using eq 3 was observed to be in the range of 10^{-1}−10^{-4}. The average apparent activation energies obtained were 207.2, 158.9, and 179.7 kJ mol^{-1} for the TV PCB, MB PCB, and HD PCB, respectively. For the TV PCB, the apparent activation energy varied in the range of 120−297 kJ mol^{-1}, while for the MB PCB, it varied from 124 to 315 kJ mol^{-1} in the conversion range of 0.15−0.6. For the HD PCB,

https://doi.org/10.1021/acsomega.2c02003
ACS Omega 2022, 7, 31713−31725

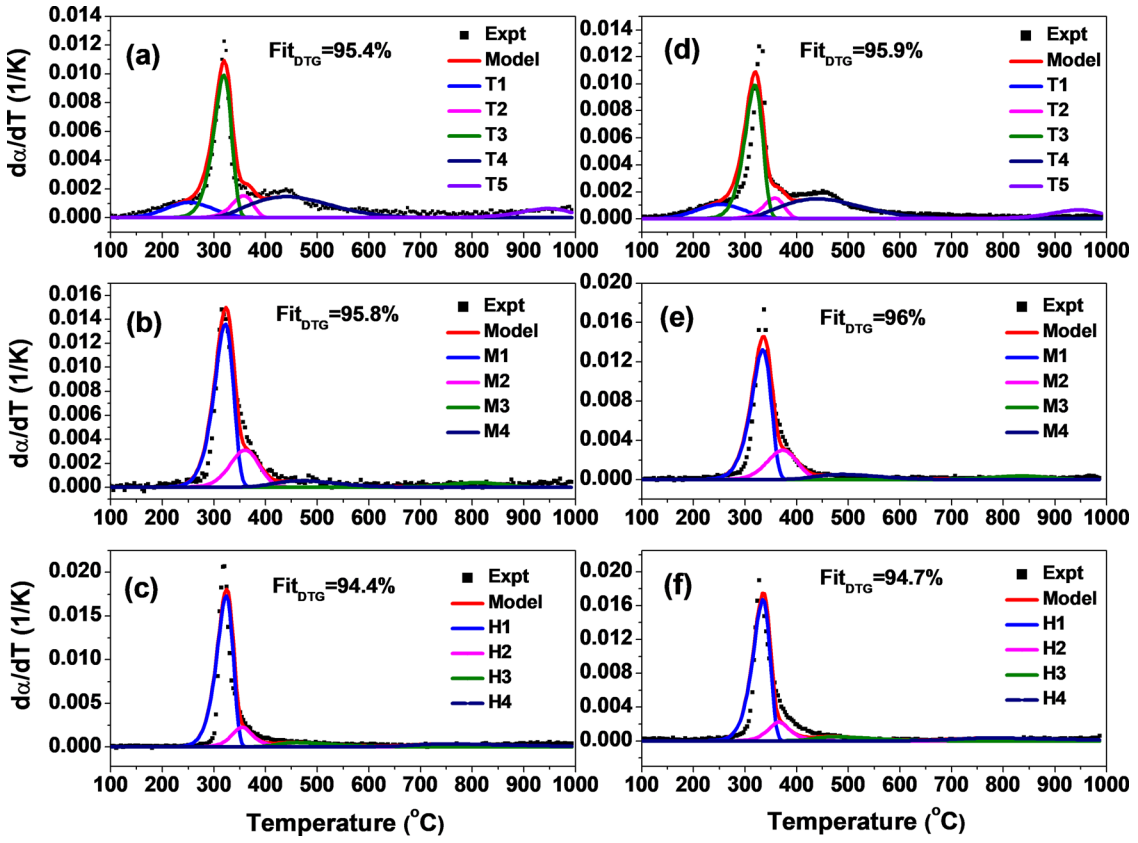

Figure 3. Experimental and simulated DTG curves at 10 °C min^{-1} for (a) TV PCB, (b) MB PCB, and (c) HD PCB. Experimental and predicted DTG curves at 20 °C min^{-1} for (d) TV PCB, (e) MB PCB, and (f) HD PCB. The decomposition curves of the individual pseudo-components are also shown in each case.

the apparent activation energy varied from 109 to 208 kJ mol^{-1} in the conversion range of 0.1−0.5, and it then decreased to 152 kJ mol^{-1} at a conversion of 0.6. This decrease in activation energy at higher conversions can be attributed, at least partially, to the formation of low-molecular weight gases, particularly HBr. Kim et al.[46] proposed a reaction pathway where the transformation of intermediates to char is followed by a concomitant increase in the concentration of HBr at high temperatures. Gautam et al.[47] carried out a kinetic analysis on the pyrolysis of nitrogen-rich species and reported low activation energies at high temperatures and ascribed this phenomenon to the catalyzing effect of metals present in the sample matrix. It is worthwhile to mention that there is a significant variation of apparent activation energy with respect to conversion for all the three PCB samples, which signifies the multistep decomposition mechanism. Owing to the global nature of the activation energy derived from the isoconversional model, the catalytic role of metals is only a speculation. To gain a better understanding of the pyrolysis mechanism of PCBs, it is important to analyze the TG and DTG profiles using a comprehensive DAEM, which is discussed in the subsequent section.

4.2.2. DAEM. The decomposition kinetics of complex mixtures can be precisely modeled using a DAEM. The DTG data obtained from TGA experiments conducted at 10 °C min^{-1} were used to estimate the kinetic parameters. Using the kinetic parameters obtained through simulations at 10 °C min^{-1}, the experimental DTG profile at 20 °C min^{-1} was predicted. The optimized parameters that best describe both the experimental DTG and experimental conversion data were considered. The number of pseudo-components considered for the TV PCB, MB PCB, and HD PCB was five, four, and four, respectively. Four pseudo-components generally describe the thermal decomposition of the PCB's organic fraction, while the fifth pseudo-component represents the char decomposition in the temperature range of 600−1000 °C. It can be observed from Figures 3 and 4 that there is a close agreement between experimental and model DTG curves and experimental and model conversion profiles at 10 and 20 °C min^{-1}. The number of pseudo-components assumed can be validated from the fit %, which is greater than 95% for both DTG and conversion plots.

The mixture of Gaussian and Weibull distributions was employed to capture all the possible reactions occurring during the course of the PCB decomposition. For the TV PCB, the number of Gaussian and Weibull distributions considered was three and two, respectively. The first Gaussian was considered in the temperature range of 100−300 °C with a temperature of maxima around 250−260 °C. This Gaussian considers the production of carbon dioxide and water moieties from the epoxy resin. The second and third Gaussians were considered in the temperature range of 250−350 and 300−400 °C, respectively. The decomposition of the TV PCB in the temperature range of 350−600 and 600−1000 °C was modeled using Weibull distribution due to the significant asymmetry observed in these regions. In fact, the use of Gaussian distribution to model the decomposition of all the pseudo-components resulted in poor fits that were lower than 85% for all the PCB samples.

https://doi.org/10.1021/acsomega.2c02003
ACS Omega 2022, 7, 31713−31725

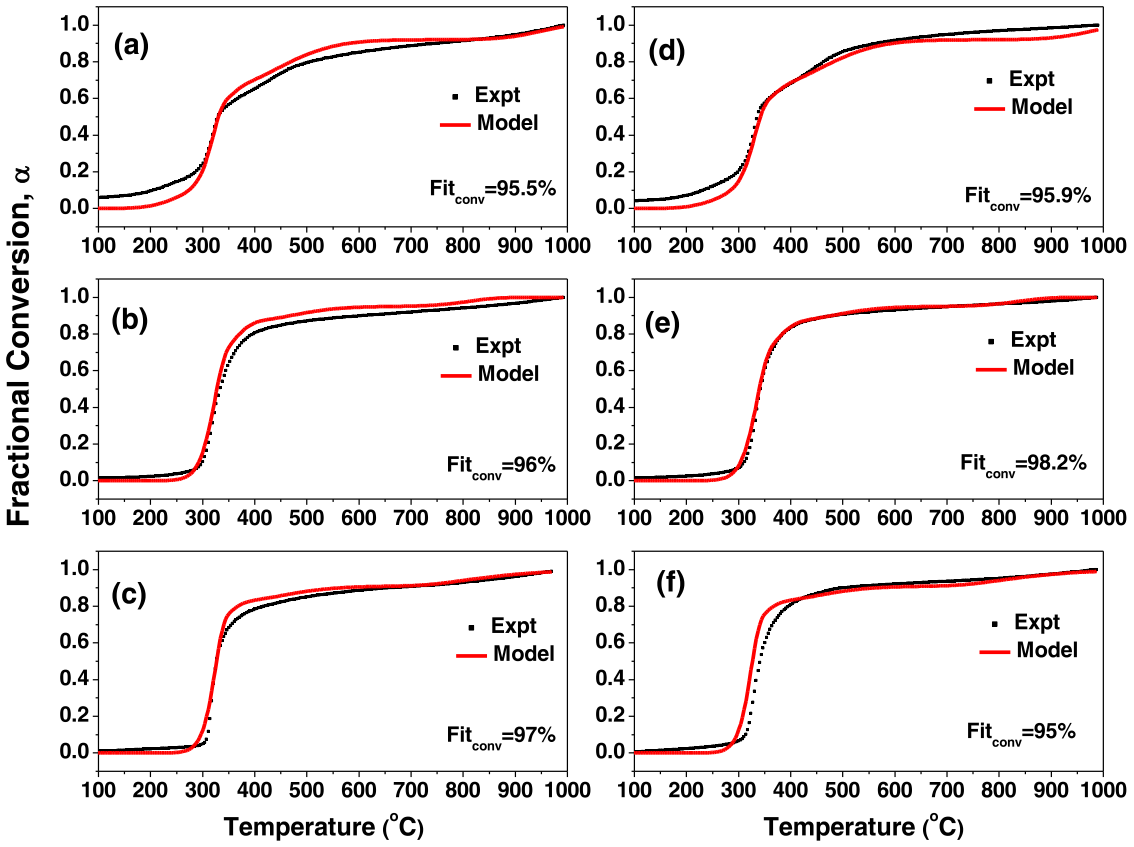

Figure 4. Experimental and simulated conversion curves at 10 °C min^{-1} for (a) TV PCB, (b) MB PCB, and (c) HD PCB. Experimental and predicted conversion curves at 20 °C min^{-1} for (d) TV PCB, (e) MB PCB, and (f) HD PCB.

Table 3. Kinetic Parameters of Decomposition of Pseudo-Components of PCB Samples Obtained from Optimization

pseudo-components	c_j	A (s^{-1})	γ (kJ mol^{-1})	ϕ	η (kJ mol^{-1})	E_o (kJ mol^{-1})	σ (kJ mol^{-1})
			TV PCB				
T1	0.12	4.5×10^8				110	8.4
T2	0.44	4×10^{13}				177	1.5
T3	0.08	8.2×10^{12}				181	2.5
T4	0.28	2×10^{14}	184	2.2	55	233	23.5
T5	0.08	1×10^9	228	7	35	261	5.5
			MB PCB				
M1	0.65	1×10^{12}				160	1
M2	0.22	1.5×10^{12}				174	5.5
M3	0.08	1×10^{12}	181	2	33	210	15.3
M4	0.05	3×10^9	205	7	45	247	7.1
			HD PCB				
H1	0.71	2×10^{14}				186	0.4
H2	0.13	5.5×10^{14}	197	0.9	7	204	8.2
H3	0.07	3×10^{13}	202	1.5	30	229	18.4
H4	0.09	4.2×10^9	215	1.8	42	225	21

The waste PCB samples comprise both brominated epoxy resins (BERs) and nonbrominated epoxy resins (NBERs). The overlapping of the peaks is mainly due to the simultaneous decomposition of BERs and NBERs. It was found that the decomposition regime of BERs lies at 250−350 °C, while NBERs decomposed in a wider temperature range of 250−500 °C.[46] From Table 3, it can be observed that the values of the shape factor (ϕ) for pseudo-components T4 and T5 are 2.2 and 7, respectively. The value of 2.2, which is obtained through simulations, indicates that the chosen Weibull distribution is positively skewed and bears a right tail. On the other hand, the value of 7 indicates that those sets of reactions can be well modeled using a negatively skewed distribution. The pseudo-components T2 and T3 represent the formation of HBr and brominated aromatics from the decomposition of flame retardants present in the TV PCB, respectively, while the pseudo-component T4 considers a range of compounds produced from the decomposition of epoxy resin of the PCB sample. The decomposition of char is represented by the fifth pseudo-component T5. The volatiles (c_j) produced by each of these pseudo-components are also shown in Table 3.

https://doi.org/10.1021/acsomega.2c02003
ACS Omega 2022, 7, 31713−31725

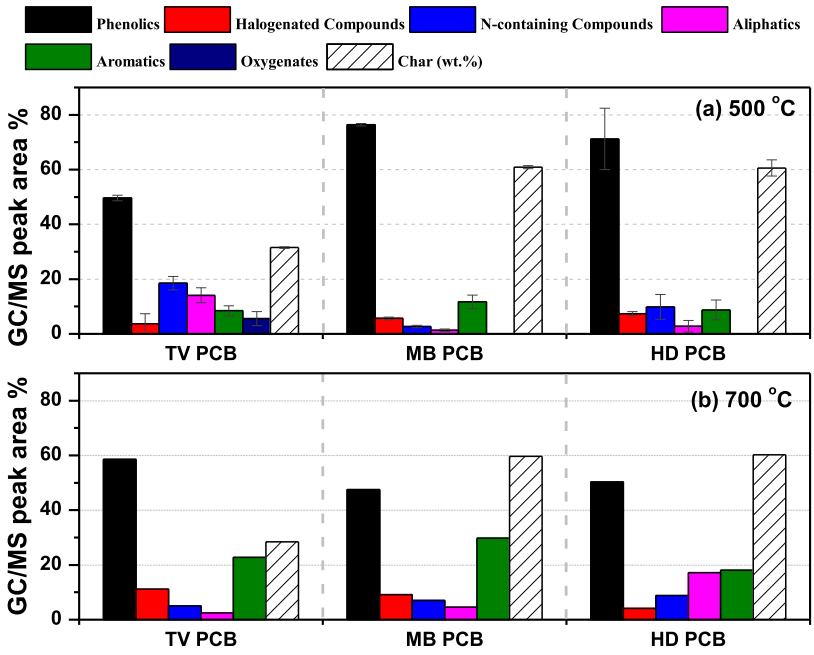

Figure 5. Selectivity of pyrolysates obtained from Py-GC/MS of treated PCB samples at (a) 500 °C and (b) 700 °C. The char yield is reported in wt %.

For the MB PCB and HD PCB, significant decomposition was not observed in the initial temperature range of 100−300 °C. Hence, no pseudo-component is considered in this region. The pseudo-components M1, M2, H1, and H2 are similar to the pseudo-components T2 and T3 of the TV PCB. Likewise, M3 and H3 are similar to T4, while M4 and H4 are similar to T5 in terms of the class of compounds being decomposed in those temperature regimes. The DAEM results provide accurate values of the statistical and kinetic parameters for the pyrolysis of these PCB samples, which aid in a better understanding of the decomposition of a heterogeneous PCB mixtures, and in accurately developing models for PCB pyrolysis that can have far-reaching applications in process-modeling suites. The mean activation energies of the TV PCB, MB PCB, and HD PCB fall in the range of 110−261, 160−247, and 186−225 kJ mol^{-1}, respectively. These values are closer to those obtained by Chen et al.[21] who reported the activation energy to vary from 80.9 to 240.5 kJ mol^{-1} for the nonmetallic fraction of waste PCBs. The values of mean activation energies and pre-exponential factors of the pseudo-components described by the Gaussian distribution are in line with those of Krishna et al.[22] for PCB pyrolysis. Liu et al.[48] studied the pyrolysis kinetics of Cu-free PCBs (CFPCBs) using the FWO method. The authors describe the decomposition of CFPCBs using four stages of decomposition. The first stage is observed for α <0.075, which is characterized by breakage of N-containing cross-linkages where low boiling products are formed. The second stage observed for $0.075 < \alpha < 0.85$ is characterized by the formation of BERs and NBERs. The decomposition of NBERs is characterized by the third stage for $0.85 < \alpha < 0.9$. The formation of char is characterized as the fourth stage for $\alpha > 0.9$. The apparent activation energy in the first stage observed by authors in this study was 119 kJ mol^{-1}. In the second stage, the apparent activation energy increased steadily from 119 to 357 kJ mol^{-1}. The apparent activation energy decreased to 279 kJ mol^{-1} in the third stage, while in the fourth stage, it grew rapidly and reached a high value of 516 kJ mol^{-1}. The pyrolysis kinetics of the FR4 PCB with and without metals was studied by Liu et al.[49] The activation energy evaluated using the Kissinger−Akahira−Sunose (KAS) method for metal-free PCBs was in the range of 96−396 kJ mol^{-1} in the conversion range of 0.05−0.8. Chen et al.[50] studied the pyrolysis kinetics of waste PCBs (WPCBs) using a discrete DAEM and observed the activation energy to vary from 49 to 203 kJ mol^{-1} for α = 0.01−0.84, while it decreased to 135 kJ mol^{-1} for α = 0.84−0.99. It was observed that the activation energies reported by authors using isoconversional methods such as FWO and KAS are very high especially at high conversions. Nonetheless, the activation energies obtained in this study through a DAEM are in reasonable bounds with the highest activation energy observed at 261 kJ mol^{-1} for decomposition of char in TV PCB samples. This implies that the DAEM approach is more accurate and robust in estimating kinetic parameters and captures the pyrolysis behavior both from conversion and DTG profiles in the entire temperature range of the study.

4.3. Analytical Fast Pyrolysis of PCBs. From the TGA graphs, it is clear that the decomposition of all the samples, viz., HD PCB, TV PCB, and MB PCB, is complete well within 500 °C. From the mass loss data, it is also evident that the TV PCB exhibited a minor mass loss even until 700−800 °C. Hence, the temperatures of 500 and 700 °C were chosen for analytical Py-GC/MS experiments. Even though the heating rate of the sample is high in Py-GC/MS as compared to that in TGA, it is meant to provide complementary information of the pyrolysis product distribution from the PCB samples. The pyrolysates from these PCB samples were categorized as phenolics, nitrogen-containing compounds, aliphatics, halogenated compounds, and aromatic hydrocarbons. The list of all compounds obtained from pyrolysis of PCB samples at 500 °C is provided in Tables S1−S3 (Supporting Information). The percentage selectivity of pyrolysates obtained from pyrolysis of treated PCB samples at 500 °C is shown in Figure 5a. The major products obtained from the TV PCB, MB PCB, and HD

https://doi.org/10.1021/acsomega.2c02003
ACS Omega 2022, 7, 31713−31725

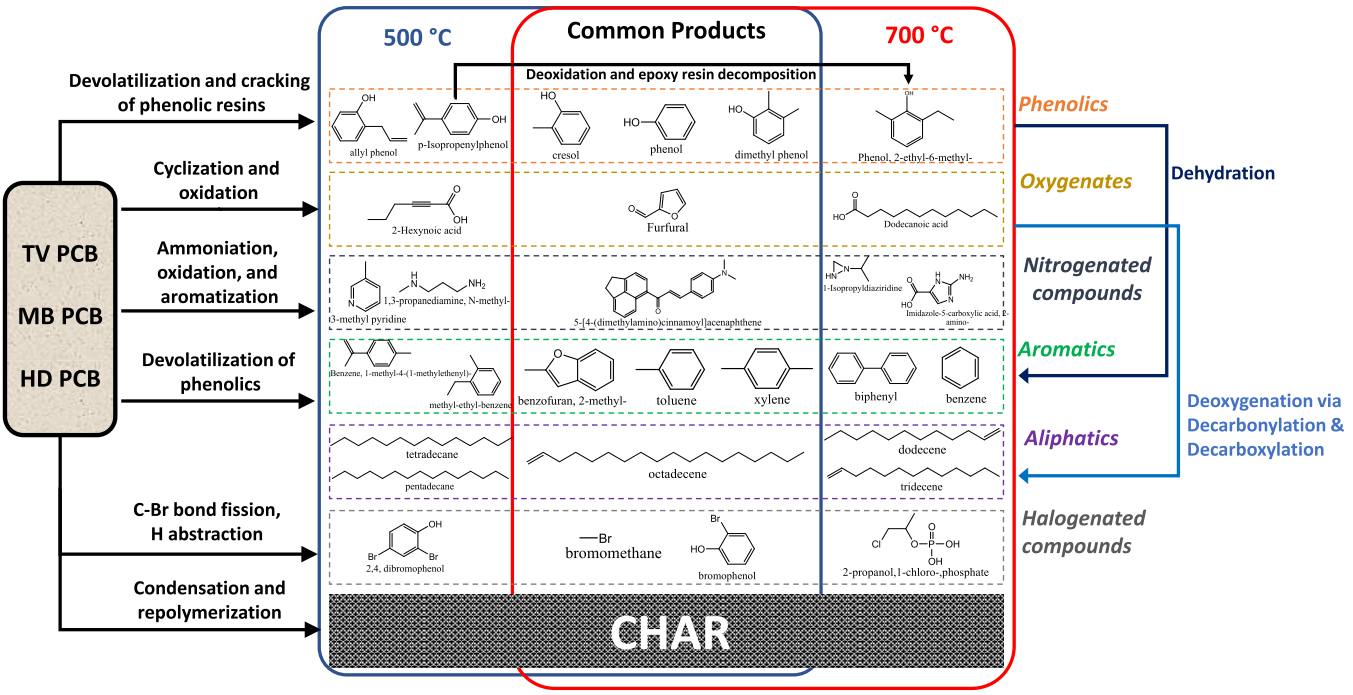

Figure 6. Schematic of the different reaction steps involved in PCB pyrolysis along with the salient organic compounds obtained from Py-GC/MS.

PCB belong to the class of phenolic derivatives. The TV PCB yielded 49.6% of phenolic derivatives, of which the selectivity to simple phenols is 24%. The specific phenols include *p*-cresol (6.8%), 2,4-dimethyl phenol (7.2%), and 2-methyl-phenol (6.7%). The selectivities to other classes of compounds were 18.5% for N-containing compounds, 14% for aliphatics, 8.4% for aromatics, 5.6% for linear and cyclic oxygenates, and 3.7% for halogenated compounds.

The Py-GC/MS results of the MB PCB show that phenolic compounds occupy a significant fraction of their structure. The selectivity to phenolics is 76% in the MB PCB. This is followed by aromatics (11.7%) and halogenated compounds (5.7%). The production of N-containing compounds and aliphatics was low with only 2.7 and 1.4%, respectively. The pyrolysate composition from the HD PCB was similar to that from the MB PCB. The selectivity of phenolics, N-containing compounds, aromatics, halogenated compounds, and aliphatics was observed to be 71, 9.8, 8.7, 7.3, and 2.8%, respectively. However, the major difference in the pyrolysis behaviors of the MB PCB and HD PCB can be observed in the selectivity of individual compounds. The major phenolic derivatives in the MB PCB include simple phenols, *p*-isopropenylphenol, and 4-(1-methylethyl)-phenol with selectivities of 36.5, 29, and 6.2%, respectively. On the other hand, the major phenolic derivatives from the HD PCB were simple phenols (51.9%), 4-(1-methylethyl)-phenol (6.2%), *p*-Isopropenylphenol (3%), and 2-methyl-phenol (3.2%).

The typical reaction steps involved in the pyrolysis of PCB samples leading to the formation of different products and the salient transformations at high temperatures are depicted in Figure 6. The decomposition of the epoxy resin matrix results in the formation of a variety of phenols and their derivatives, while the decomposition of cellulosic pressboard fibers results in the formation of furfural. Ammoniation and aromatization reactions result in the formation of condensed ring aromatics and N-containing aromatics. The secondary transformation of phenolics via dehydration and deoxygenation results in aromatic hydrocarbons. To understand the effect of the temperature on PCB pyrolysis, Py-GC/MS experiments were conducted at 700 °C (Figure 5b). Tables S4−S6 (Supporting Information) present the list of various compounds that evolved at 700 °C from the pyrolysis of the PCB samples. It is evident that the selectivity to phenolics reduced significantly in the case of the MB PCB and HD PCB (71−76 to 48−50%), while it increased from ∼50 to 58% for the TV PCB as the temperature was increased. The char yields at 500 and 700 °C were almost similar for the MB PCB and HD PCB, while there was a slight mass loss of 3 wt % for the TV PCB. These results suggest that there is a possibility of deoxygenation occurring at higher temperatures in the case of the MB PCB and HD PCB, which results in a decline in the selectivity to phenolics with a concomitant increase in the selectivity to aromatics.

The deoxygenation can be possibly due to the higher energy being supplied at 700 °C and also due to the catalytic role of copper present in these samples (Table 2). The aromatic compounds observed at 700 °C include benzene, toluene, ethylbenzene, and styrene. The formation of long-chain alkanes and alkenes at 700 °C can also be attributed to deoxygenation via decarboxylation and decarbonylation of fatty acids and carbonyl compounds. In the case of the TV PCB, it can be speculated that phenolics have transformed into aromatics through dehydration, and the higher extent of conversion, evidenced by a greater mass loss, can be due to further decomposition of epoxy resin to phenolic derivatives. This result can also be validated with the mass loss observed at 700 °C from TGA experiments for the TV PCB; unlike this, the sample mass was almost constant for the MB PCB and HD PCB as the temperature was increased from 500 to 700 °C. Furthermore, the selectivity to 3,3,5-trimethyl-cyclohexene decreased from 11.9% at 500 °C to 5.6% at 700 °C. On the other hand, at 700 °C, the formation of 1-tridecene was observed with a selectivity of 5.3%. This concomitant decrease in the selectivity of cyclo-alkene with a subsequent increase in the selectivity of straight-chain alkenes can be attributed to the

https://doi.org/10.1021/acsomega.2c02003
ACS Omega 2022, 7, 31713−31725

ring opening of cyclic hydrocarbons via C−C bond fission reactions that may become dominant at high temperatures. Overall, it can be concluded that pyrolysis is a promising pretreatment strategy to recover the plastic fraction of e-wastes either before or after the recovery of the metallic fraction.

5. CONCLUSIONS

This study presents the kinetic analysis and various chemical functionalities obtained from pyrolysis of three PCBs, viz., TV PCB, MB PCB, and HD PCB. The following conclusions were derived from analyzing the results of the study:

- Acid pretreatment of the PCB samples resulted in the significant removal of copper along with the complete removal of aluminum, iron, nickel, lead, and tin from the PCBs.
- The average apparent activation energies obtained from the Vyazovkin method were 207.2, 158.9, and 179.7 kJ mol^{-1} for the TV, MB, and HD PCBs, respectively.
- The DAEM with two different distributions (Gaussian and Weibull) accurately predicted the thermogravimetric mass loss and differential mass loss profiles. The mean activation energies of decomposition of the pseudo-components belonging to the TV PCB, MB PCB, and HD PCB were observed to be in the range of 110−261, 160−247, and 186−225 kJ mol^{-1}, respectively, while the pre-exponential factors varied in the range of 10^8−10^{14} s^{-1} for all three PCBs.
- The DAEM developed using multiple distributions in this study is shown to be a robust kinetic strategy to describe the pyrolysis of heterogeneous and complex mixtures like PCBs.
- The fast pyrolysis of PCB samples conducted at 500 and 700 °C showed that the major class of compounds obtained from pyrolysis was phenolics. However, at 700 °C, the selectivity to phenolic derivatives decreased with the pyrolysis of MB and HD PCBs with a concomitant increase in selectivity to aromatics, suggesting that deoxygenation is a possible reaction pathway.
- In the case of the TV PCB, ring opening of cycloalkenes was observed at 700 °C, which subsequently led to the production of straight-chain alkenes. The plausible reaction steps involved in the formation of different pyrolysates were identified and proposed.

■ ASSOCIATED CONTENT

Supporting Information

The Supporting Information is available free of charge at https://pubs.acs.org/doi/10.1021/acsomega.2c02003.

Thermogravimetric (TG) mass loss and differential thermogravimetric (DTG) curves for the TV PCB, MB PCB, and HD PCB at different heating rates (20, 30, 40 °C min^{-1}) and Py-GC/MS pyrolysate composition from the TV PCB, MB PCB, and HD PCB at 500 and 700 °C (PDF)

■ AUTHOR INFORMATION

Corresponding Author

Ravikrishnan Vinu − *Department of Chemical Engineering, Indian Institute of Technology Madras, Chennai 600036 Tamil Nadu, India;* orcid.org/0000-0002-9757-8225; Phone: +91-44-22574187; Email: vinu@smail.iitm.ac.in

Authors

Jonnalagedda Varaha Jayarama Krishna − *Department of Chemical Engineering, Indian Institute of Technology Madras, Chennai 600036 Tamil Nadu, India*

Peter Francis Prashanth − *Department of Chemical Engineering, Indian Institute of Technology Madras, Chennai 600036 Tamil Nadu, India*

Complete contact information is available at: https://pubs.acs.org/10.1021/acsomega.2c02003

Notes

The authors declare no competing financial interest.

■ ACKNOWLEDGMENTS

The authors thank the National Center for Combustion Research and Development (NCCRD), funded by the Department of Science and Technology (DST), India, for providing access to the Pyroprobe-GC/MS facility.

■ NOMENCLATURE

A = pre-exponential (or frequency) factor (s^{-1})
c_j = mass fraction of *the* j-th pseudo-component
E_a = activation energy (kJ mol^{-1})
E_o = mean activation energy (kJ mol^{-1})
$f(E)$ = activation energy distribution function (mol kJ^{-1})
$f(\alpha)$ = reaction model
$g(\alpha)$ = integral reaction model
$I(E,T)$ = temperature integral
n = number of heating rates
n_d = number of data points used
R = universal gas constant (kJ mol^{-1} K^{-1})
S = objective function for differential thermogravimetric data (K^{-2})
S^1 = objective function for conversion data
T = temperature (K)
T_o = initial temperature (K)
T_p = temperature of maximum decomposition (K)
α = extent of conversion
β = linear heating rate (K min^{-1} or °C min^{-1})
γ = location parameter of the Weibull distribution (kJ mol^{-1})
η = scale parameter of the Weibull distribution (kJ mol^{-1})
ϕ = shape parameter of the Weibull distribution
σ = standard deviation of the activation energy distribution (kJ mol^{-1})

■ REFERENCES

(1) United Nations Institute for Training and Research, http://ewastemonitor.info/ (accessed on April 2022).

(2) E-waste: A growing problem. https://www.businesstoday.in/zero-carbon-challenge/story/e-waste-a-growing-problem-295647-2021-05-12 (accessed on June 2022).

(3) Wang, Q.; Zhang, B.; Yu, S.; Xiong, J.; Yao, Z.; Hu, B.; Yan, J. Waste-Printed Circuit Board Recycling: Focusing on Preparing Polymer Composites and Geopolymers. *ACS Omega* **2020**, *5*, 17850−17856.

(4) Guo, J.; Guo, J.; Xu, Z. Recycling of Non-Metallic Fractions from Waste Printed Circuit Boards: A Review. *J. Hazard. Mater.* **2009**, *168*, 567−590.

(5) He, W.; Li, G.; Ma, X.; Wang, H.; Huang, J.; Xu, M.; Huang, C. WEEE Recovery Strategies and the WEEE Treatment Status in China. *J. Hazard. Mater.* **2006**, *136*, 502−512.

(6) Gurgul, A.; Szczepaniak, W.; Zabłocka-Malicka, M. Incineration, Pyrolysis and Gasification of Electronic Waste. In *E3S Web of*

Conferences, 2017, Vol. *22*, p 00060. DOI: DOI: 10.1051/e3sconf/20172200060.
(7) Ikhlayel, M. Environmental Impacts and Benefits of State-of-the-Art Technologies for E-Waste Management. *Waste Manage.* **2017**, *68*, 458−474.
(8) Pihl, O.; Khaskhachikh, V.; Kravetskaja, J.; Niidu, A.; Siirde, A. Co-Pyrolysis of Estonian Oil Shale with Polymer Wastes. *ACS Omega* **2021**, *6*, 31658−31666.
(9) Zhang, J.; Sekyere, D. T.; Niwamanya, N.; Huang, Y.; Barigye, A.; Tian, Y. Study on the Staged and Direct Fast Pyrolysis Behavior of Waste Pine Sawdust Using High Heating Rate TG-FTIR and Py-GC/MS. *ACS Omega* **2022**, *7*, 4245−4256.
(10) Torres, E.; Rodriguez-Ortiz, L. A.; Zalazar, D.; Echegaray, M.; Rodriguez, R.; Zhang, H.; Mazza, G. 4-E (Environmental, Economic, Energetic and Exergetic) Analysis of Slow Pyrolysis of Lignocellulosic Waste. *Renewable Energy* **2020**, *162*, 296−307.
(11) Shen, Y.; Chen, X.; Ge, X.; Chen, M. Chemical Pyrolysis of E-Waste Plastics: Char Characterization. *J. Environ. Manage.* **2018**, *214*, 94−103.
(12) Kantarelis, E.; Yang, W.; Blasiak, W.; Forsgren, C.; Zabaniotou, A. Thermochemical Treatment of E-Waste from Small Household Appliances Using Highly Pre-Heated Nitrogen-Thermogravimetric Investigation and Pyrolysis Kinetics. *Appl. Energy* **2011**, *88*, 922−929.
(13) Suriapparao, D. V.; Batchu, S. P.; Jayasurya, S.; Vinu, R. Selective Production of Phenolics from Waste Printed Circuit Boards via Microwave Assisted Pyrolysis. *J. Cleaner Prod.* **2018**, *197*, 525−533.
(14) Vyazovkin, S.; Burnham, A. K.; Criado, J. M.; Pérez-Maqueda, L. A.; Popescu, C.; Sbirrazzuoli, N. ICTAC Kinetics Committee Recommendations for Performing Kinetic Computations on Thermal Analysis Data. *Thermochim. Acta* **2011**, *520*, 1−19.
(15) Bui, H. H.; Tran, K. Q.; Chen, W. H. Pyrolysis of Microalgae Residues - A Kinetic Study. *Bioresour. Technol.* **2016**, *199*, 362−366.
(16) Carrier, M.; Loppinet-Serani, A.; Denux, D.; Lasnier, J. M.; Ham-Pichavant, F.; Cansell, F.; Aymonier, C. Thermogravimetric Analysis as a New Method to Determine the Lignocellulosic Composition of Biomass. *Biomass Bioenergy* **2011**, *35*, 298−307.
(17) Kim, Y. M.; Han, T. U.; Watanabe, C.; Teramae, N.; Park, Y. K.; Kim, S.; Hwang, B. Analytical Pyrolysis of Waste Paper Laminated Phenolic-Printed Circuit Board (PLP-PCB). *J. Anal. Appl. Pyrolysis* **2015**, *115*, 87−95.
(18) Rodriguez, R.; Mazza, G.; Fernandez, A.; Saffe, A.; Echegaray, M. Prediction of the Lignocellulosic Winery Wastes Behavior during Gasification Process in Fluidized Bed: Experimental and Theoretical Study. *J. Environ. Chem. Eng.* **2018**, *6*, 5570−5579.
(19) Fernandez, A.; Palacios, C.; Echegaray, M.; Mazza, G.; Rodriguez, R. Pyrolysis and Combustion of Regional Agro-Industrial Wastes: Thermal Behavior and Kinetic Parameters Comparison. *Combust. Sci. Technol.* **2018**, *190*, 114−135.
(20) Hao, J.; Wang, H.; Chen, S.; Cai, B.; Ge, L.; Xia, W. Pyrolysis Characteristics of the Mixture of Printed Circuit Board Scraps and Coal Powder. *Waste Manage.* **2014**, *34*, 1763−1769.
(21) Chen, Y.; Yang, J.; Zhang, Y.; Liu, K.; Liang, S.; Xu, X.; Hu, J.; Yao, H.; Xiao, B. Kinetic Simulation and Prediction of Pyrolysis Process for Non-Metallic Fraction of Waste Printed Circuit Boards by Discrete Distributed Activation Energy Model Compared with Isoconversional Method. *Environ. Sci. Pollut. Res.* **2018**, *25*, 3636−3646.
(22) Krishna, J. V. J.; Damir, S. S.; Vinu, R. Pyrolysis of Electronic Waste and Their Mixtures: Kinetic and Pyrolysate Composition Studies. *J. Environ. Chem. Eng.* **2021**, *9*, No. 105382.
(23) Quan, C.; Li, A.; Gao, N. Research on Pyrolysis of PCB Waste with TG-FTIR and Py-GC/MS. *J. Therm. Anal. Calorim.* **2012**, *110*, 1463−1470.
(24) Duan, H.; Li, J. Thermal Degradation Behavior of Waste Video Cards Using Thermogravimetric Analysis and Pyrolysis Gas Chromatography/Mass Spectrometry Techniques. *J. Air Waste Manage. Assoc.* **2010**, *60*, 540−547.
(25) Torres-Sciancalepore, R.; Fernandez, A.; Asensio, D.; Riveros, M.; Fabani, M. P.; Fouga, G.; Rodriguez, R.; Mazza, G. Kinetic and Thermodynamic Comparative Study of Quince Bio-Waste Slow Pyrolysis before and after Sustainable Recovery of Pectin Compounds. *Energy Convers. Manag.* **2022**, *252*, No. 115076.
(26) Gande, V. V.; Vats, S.; Bhatt, N.; Pushpavanam, S. Sequential recovery of metals from waste printed circuit boards using a zero-discharge hydrometallurgical process. *Cleaner Eng. Technol.* **2021**, *4*, No. 100143.
(27) Jayarama Krishna, J.; Korobeinichev, O. P.; Vinu, R. Isothermal fast pyrolysis kinetics of synthetic polymers using analytical Pyroprobe. *J. Anal. Appl. Pyrol.* **2019**, *139*, 48−58.
(28) Ojha, D. K.; Viju, D.; Vinu, R. Fast pyrolysis kinetics of alkali lignin: Evaluation of apparent rate parameters and product time evolution. *Bioresour. Technol.* **2017**, *241*, 142−151.
(29) Venkatesan, K.; Prashanth, F.; Kaushik, V.; Choudhari, H.; Mehta, D.; Vinu, R. Evaluation of pressure and temperature effects on hydropyrolysis of pine sawdust: pyrolysate composition and kinetic studies. *React. Chem. Eng.* **2020**, *5*, 1484−1500.
(30) Ojha, D. K.; Viju, V.; Vinu, R. Fast pyrolysis kinetics of lignocellulosic biomass of varying compositions. *Energy Convers. Manag.: X* **2021**, *10*, No. 100071.
(31) Jie, G.; Ying-Shun, L.; Mai-Xi, L. Product Characterization of Waste Printed Circuit Board by Pyrolysis. *J. Anal. Appl. Pyrolysis* **2008**, *83*, 185−189.
(32) Caballero, B. M.; de Marco, I.; Adrados, A.; López-Urionabarrenechea, A.; Solar, J.; Gastelu, N. Possibilities and Limits of Pyrolysis for Recycling Plastic Rich Waste Streams Rejected from Phones Recycling Plants. *Waste Manage.* **2016**, *57*, 226−234.
(33) Kumagai, S.; Grause, G.; Kameda, T.; Yoshioka, T. Thermal Decomposition of Tetrabromobisphenol-A Containing Printed Circuit Boards in the Presence of Calcium Hydroxide. *J. Mater. Cycles Waste Manage.* **2017**, *19*, 282−293.
(34) Khawam, A.; Flanagan, D. R. Basics and Applications of Solid-State Kinetics: A Pharmaceutical Perspective. *J. Pharm. Sci.* **2006**, *95*, 472−498.
(35) Parthasarathy, P.; Fernandez, A.; Al-Ansari, T.; Mackey, H. R.; Rodriguez, R.; McKay, G. Thermal Degradation Characteristics and Gasification Kinetics of Camel Manure Using Thermogravimetric Analysis. *J. Environ. Manage.* **2021**, *287*, No. 112345.
(36) Cai, J.; Wu, W.; Liu, R.; Huber, G. W. A Distributed Activation Energy Model for the Pyrolysis of Lignocellulosic Biomass. *Green Chem.* **2013**, *15*, 1331−1340.
(37) Viju, D.; Gautam, R.; Vinu, R. Application of the Distributed Activation Energy Model to the Kinetic Study of Pyrolysis of *Nannochloropsis oculata*. *Algal Res.* **2018**, *35*, 168−177.
(38) Shen, D. K.; Gu, S.; Jin, B.; Fang, M. X. Thermal Degradation Mechanisms of Wood under Inert and Oxidative Environments Using DAEM Methods. *Bioresour. Technol.* **2011**, *102*, 2047−2052.
(39) Cai, J.; Wu, W.; Liu, R. An Overview of Distributed Activation Energy Model and Its Application in the Pyrolysis of Lignocellulosic Biomass. *Renewable Sustainable Energy Rev.* **2014**, *36*, 236−246.
(40) Burra, K. G.; Gupta, A. K. Kinetics of synergistic effects in co-pyrolysis of biomass with plastic wastes. *Appl. Energy* **2018**, *220*, 408−418.
(41) Cai, J. M.; Liu, R. H. Parametric Study of the Nonisothermal n-th Order Distributed Activation Energy Model Involved the Weibull Distribution for Biomass Pyrolysis. *J. Therm. Anal. Calorim.* **2007**, *89*, 971−975.
(42) Cai, J. M.; Liu, R. H. New Approximation for the General Temperature Integral. *J. Therm. Anal. Calorim.* **2007**, *90*, 469−474.
(43) Eberhart, R. C.; Shi, Y.Particle Swarm Optimization: Developments, Applications and Resources. In Proceedings of the 2001 Congress on Evolutionary Computation (IEEE Cat. No. 01TH8546), IEEE, 2001; Vol. *1*, pp 81−86. DOI: DOI: 10.1109/CEC.2001.934374.
(44) Chiang, H. L.; Lin, K. H.; Lai, M. H.; Chen, T. C.; Ma, S. Y. Pyrolysis Characteristics of Integrated Circuit Boards at Various

Particle Sizes and Temperatures. *J. Hazard. Mater.* **2007**, *149*, 151−159.
(45) Grause, G.; Furusawa, M.; Okuwaki, A.; Yoshioka, T. Pyrolysis of Tetrabromobisphenol-A Containing Paper Laminated Printed Circuit Boards. *Chemosphere* **2008**, *71*, 872−878.
(46) Kim, Y. M.; Kim, S.; Lee, J. Y.; Park, Y. K. Pyrolysis Reaction Pathways of Waste Epoxy-Printed Circuit Board. *Environ. Eng. Sci.* **2013**, *30*, 706−712.
(47) Gautam, R.; Vinu, R.; Vaithyanathan, P. Analytical Fast Pyrolysis of Nitrogen-Rich Mosquito Species via Pyrolysis-FTIR and Pyrolysis-GC/MS. *J. Anal. Appl. Pyrolysis* **2020**, *146*, No. 104766.
(48) Liu, W.; Xu, J.; Han, J.; Jiao, F.; Qin, W.; Li, Z. Kinetic and Mechanism Studies on Pyrolysis of Printed Circuit Boards in the Absence and Presence of Copper. *ACS Sustainable Chem. Eng.* **2019**, *7*, 1879−1889.
(49) Liu, J.; Jiang, Q.; Wang, H.; Li, J.; Zhang, W. Catalytic Effect and Mechanism of In-Situ Metals on Pyrolysis of FR4 Printed Circuit Boards: Insights from Kinetics and Products. *Chemosphere* **2021**, *280*, No. 130804.
(50) Chen, Y.; Liang, S.; Xiao, K.; Hu, J.; Hou, H.; Liu, B.; Deng, H.; Yang, J. A Cost-Effective Strategy for Metal Recovery from Waste Printed Circuit Boards via Crushing Pretreatment Combined with Pyrolysis: Effects of Particle Size and Pyrolysis Temperature. *J. Cleaner Prod.* **2021**, *280*, No. 124505.

https://doi.org/10.1021/acsomega.2c02003
ACS Omega 2022, 7, 31713−31725